Proceeding of the 2013
RSI/ISM International Conference on Robotics and Mechatronics
February 13-15, 2013, Tehran, Iran

UAV Guidance For Tracking Control Of Mobile Robots In Presence Of Obstacles

Azade Aghaeeyan,[1] F. Abdollahi[2] and H.A Talebi[2]

***Abstract*—In this paper, a coordination of two types of heterogeneous robots, namely unmanned aerial vehicle(UAV) and unmanned ground vehicle(UGV) is considered. The UAV plays the role of a virtual leader for the UGVs. While UAV tracks a predefined geometric path, the UGVs are supposed to make a desired formation around the planar position of UAV and avoid obstacles. UAV should be aware of its distance with mobile robots and improve its motion to keep connection among vehicles. In the next step, the UAV encounters pop-up threats, too. The simulation results validate the performance of the proposed algorithm.**
Index Terms-Quadrotor, Mobile robots, Obstacle avoidance, Multi agent systems

I. INTRODUCTION

Multi agent systems have received considerable attention in recent years. It is due to their advantages in accomplishing complex missions such as discoveries, surveillance, disaster monitoring and so on. One of the attractive scenarios for multi agent systems is formation. Indeed formation control can be considered as controlling relative position and orientation of robots in a team [1]. Formation control has been investigated in three main approaches in the literature, namely:Leader-Follower, behavioral and virtual structures. In the leader-follower approach, one agent, designed as a leader, moves along a predefined trajectory, and the other ones should maintain a desired distance and orientation to the leader [1]. In the second approach several desired behaviors e.g. obstacle avoidance, target seeking and so on are assigned to each robot. The resultant behavior of each of them is derived by weighting the relative importance of each objective [2]. In virtual structure a virtual agent is considered as a leader. The great merit of these two approaches is that the leader never fails while in leader-follower design the mission may be dismissed by a faulty leader.

Unmanned Aerial Vehicles(UAV) can observe further distances in comparison to Unmanned Ground Vehicles(UGVs), due to its peripheral vision; On the other hand, UGVs are capable to detect the ground objects more precisely [3]. Taking advantages of two types of agents yield accomplishing more complicated missions. Collaboration among heterogeneous vehicles has been enormously investigated in literature. In [4] A team of heterogeneous robots was navigated in a priori known environment with obstacles. By employing feedback linearisation, the agents' dynamics were turned to a single integrator. In [5] the UGVs synchronized their velocities and UAVs were supposed to track ground group centroid. [6] introduced the UAV as leader for a large team of nonholonomic ground vehicles. It developed an abstraction for the UGVs that allows the UAV to control them without knowing the features of individual UGVs.

Consider a scenario in which a group of UGVs are supposed to pass through an unknown environment to get to a static target. Since UAV can observe far distances and large menaces, it is considered as a leader whose path planner unit devises a safe path for UAV to achieve the target. On the other hand, because of UAV height, it can not detect the small ground obstacles from far distance. Therefore the UGVs should deploy a suitable approach to avoid the possible ground threats. Due to communication limitation there are constraints on the distance between UAV and the mobile robots. These constraints will be critical when UGVs face obstacles. As a result a proper strategy should be deployed to keep them in acceptable distances. In the next step it is assumed that the UAV may face aerial hazards and proper reaction has been proposed to cope with this problem.

The organization of this paper is as follows: In Section 2 the dynamical model of UAV and UGVs are given and proper formation control is introduced. In section 3 obstacle avoidance has been investigated. Section 4 provides simulation results and finally the conclusions are given in Section 5.

II. AGENTS MODEL AND CONTROL

A. UAV Model And Control

In this paper, a quadrotor is considered as aerial vehicle. Since rotor craft can monoeuver sharply and hover precisely. On the other hand fixed-wing air crafts have constraint on their minimum velocity which is more than the maximum velocity of the mobile robots. Therefore fixed-wing aircrafts and mobile robots can not make a formation unless UAV rotates around the center of formation.

Quadrotors have been inherited two rotorcraft characteristics: under actuation and strong coupling in pitch-yaw and roll. The quadrotor modeling and control has been enormously investigated in the literature [7].

[1]A. Aghaeeyan is the M. Sc, Student of the Department of Electrical Engineering, Amirkabir University of Technology (Tehran Polytechnic), Tehran, Iran, aghaeeyan @ aut.ac.ir

[2]F. Abdollahi and H.A Talebi are with the Department of Electrical Engineering, Amirkabir University of Technology (Tehran Polytechnic), Tehran, Iran, f_abdollahi@ aut.ac.ir

978-1-4673-5811-8/13/$31.00

A quadrotor can be modeled by following equations [8]

$$\begin{cases} \ddot{\phi} = \dot{\theta}\dot{\psi}\frac{(I_y - I_z)}{I_x} - \frac{J_r}{I_x}\dot{\theta}\Omega + \frac{l}{I_x}U_2 \\ \ddot{\theta} = \dot{\phi}\dot{\psi}\frac{(I_z - I_x)}{I_y} + \frac{J_r}{I_y}\dot{\psi}\Omega + \frac{l}{I_y}U_3 \\ \ddot{\psi} = \dot{\phi}\dot{\theta}\frac{(I_x - I_y)}{I_z} + \frac{1}{I_z}U_3 \\ \ddot{z} = -g + (\cos\phi\cos\theta)\frac{1}{m}U_1 \\ \ddot{x} = (\cos\phi\sin\theta\cos\psi + \sin\phi\sin\psi)\frac{1}{m}U_1 \\ \ddot{y} = (\cos\phi\sin\theta\sin\psi - \sin\phi\cos\psi)\frac{1}{m}U_1 \end{cases} \quad (1)$$

where (ϕ,θ,ψ) represents the UAV rotational subsystem,

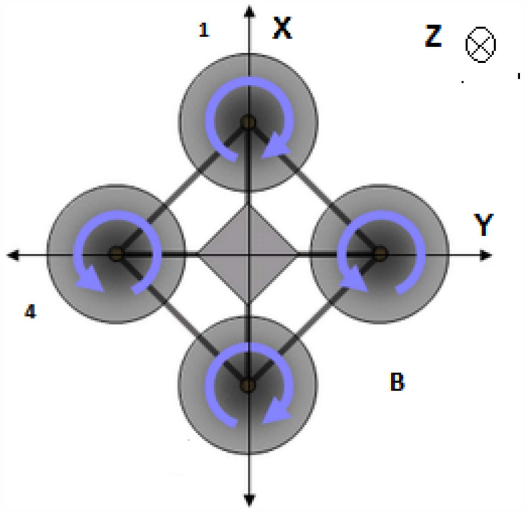

Fig. 1. Quadrotor body fixed frame

namely pitch, roll and yaw, respectively and (x,y,z) represents the Cartesian UAV position in reference frame. $I_{x,y,z}$ is the body inertia and J_r is the rotor inertia, m, and g represent robot mass and gravity respectively. Figure 1, shows the quadrotor body fixed frame and its rotor circulation direction. The system inputs are posed to U_1,U_2,U_3,U_4 and Ω a disturbance, which are obtained by:

$$\begin{cases} U_1 = b(\Omega_1^2 + \Omega_2^2 + \Omega_3^2 + \Omega_4^2) \\ U_2 = b(\Omega_4^2 - \Omega_2^2) \\ U_3 = b(\Omega_3^2 - \Omega_1^2) \\ U_4 = d(\Omega_2^2 - \Omega_4^2 - \Omega_1^2 - |\Omega_3^2) \\ \Omega = d(\Omega_2 + \Omega_4 - \Omega_1 - \Omega_3) \end{cases} \quad (2)$$

where $\Omega_i, i = 1,2,3,4$, represents the i^{th} rotor speed, b is thrust factor and, d is drag factor.

We would like to make the UAV track the desired geometric path that is denoted by (x_d,y_d,z_d). By considering equation(1), one can get its orientation subsystem is independent from position subsystem while the position subsystem dynamic is dependent on the orientation subsystem. For the sake of simplicity, let us consider $\psi_d = 0$. The following assumption is considered along this paper.

• *Assumption 1*

By assuming ψ rapidly converges to ψ_d, the 5^{th} and the 6^{th} equations in (1) can be rewrited as

$$\ddot{x} = (\cos\phi\sin\theta)\frac{1}{m}U_1$$
$$\ddot{y} = -\sin\phi\frac{1}{m}U_1$$

Thus, using the inverse kinematic, we can obtain the desired values of ϕ and θ, (ϕ_d,θ_d), such that $\phi \to \phi_d$, $\theta \to \theta_d$, implies $x \to x_d$, $y \to y_d$.

Using the back-stepping approach proposed in [8], one can synthesize the control law forcing the system to follow the desired trajectory(ψ_d, z_d, x_d, y_d), here we assume that ($\ddot{x_d}, \ddot{y_d}, \ddot{z_d}, \ddot{\psi_d}, \ddot{\theta_d}, \ddot{\phi_d}$) are equal to zero. Let us consider the tracking errors as:

$$\begin{aligned} z_1 &= \phi_d - \phi, & z_2 &= \dot{\phi} - \dot{\phi_d} - \alpha_1 z_1 \\ z_3 &= \theta_d - \theta, & z_4 &= \dot{\theta} - \dot{\theta_d} - \alpha_3 z_3 \\ z_5 &= \psi_d - \psi, & z_6 &= \dot{\psi} - \dot{\psi_d} - \alpha_5 z_5 \\ z_7 &= z_d - z, & z_8 &= \dot{z} - \dot{z_d} - \alpha_7 z_7 \\ z_9 &= x_d - x, & z_{10} &= \dot{x} - \dot{x_d} - \alpha_9 z_9 \\ z_{11} &= y_d - y, & z_{12} &= \dot{y} - \dot{y_d} - \alpha_{11} z_{11} \end{aligned}$$

and the Lyapunov function $V(z_i, z_{i+1}) = \frac{1}{2}z_i^2 + z_{i+1}^2$. Where α_i is a positive constant. Then the control inputs are extracted based on Lyapunov theorem such that make $\dot{V}_{(z_i,z_{i+1})} < 0$, as follows:

$$\begin{aligned} U_2 &= \frac{I_x}{l}(z_1 - a_1\dot{\theta}\dot{\psi} - a_2\dot{\theta}\Omega - \alpha_1(z_2 + \alpha_1 z_1) - \alpha_2 z_2) \\ U_3 &= \frac{I_y}{l}(z_3 - a_3\dot{\theta}\dot{\psi} - a_4\dot{z}\Omega - \alpha_3(z_4 + \alpha_3 z_3) - \alpha_4 z_4) \\ U_4 &= \frac{I_z}{l}(z_5 - a_5\dot{\phi}\dot{\theta} - \alpha_5(z_6 + \alpha_5(z_6 + \alpha_5 z_5) - \alpha_6 z_6) \\ U_1 &= \frac{m}{\cos\phi\cos\theta}(z_7 + g - \alpha_7(z_8 + \alpha_7 z_7) - \alpha_8 z_8) \\ u_x &= \frac{m}{U_1}(z_9 + \alpha_9(z_1 0 + \alpha_9 z_9) - \alpha_{10} z_{10}) \\ u_y &= \frac{m}{U_1}(z_{11} + \alpha_{11}(z_{12} + \alpha_{11} z_{11}) - \alpha_{12} z_{12}) \end{aligned} \quad (3)$$

where

$$\begin{aligned} a_1 &= \frac{I_y - I_z}{I_x}, & a_2 &= \frac{-J_R}{I_x} \\ a_3 &= \frac{I_z - I_x}{I_y}, & a_4 &= \frac{I_R}{I_y} \\ a_5 &= \frac{I_x - I_y}{I_z}, & u_x &= cos\phi sin\theta \\ u_y &= sin\phi \end{aligned}$$

In order to satisfy the Assumption 1; α_5 should be chosen large enough in comparison with other multipliers, $\alpha_i, i = 1,..,12$. By using the control algorithm in (3)UAV, as a leader, is able to track the desired trajectory $(x_d, y_d, z_d, \psi_d))$. Now, we consider the UGVs in the following.

B. UGVs Model And Control

Consider four unicycles vehicles modeled by following equation

$$\begin{aligned} \dot{x}_i &= V_i \cos\theta_i - L\omega_i \sin\theta_i \\ \dot{y}_i &= V_i \sin\theta_i + L\omega_i \cos\theta_i \\ \dot{\theta}_i &= \omega_i \end{aligned} \tag{4}$$

where,

- (x_i,y_i) are configuration states of the i^{th} unicycle at the point P, see Figure 2.
- (V,ω) are linear and angular velocity of the robot, respectively.
- (L,0)is the coordination of P according to local reference frame (X_b,Y_b).

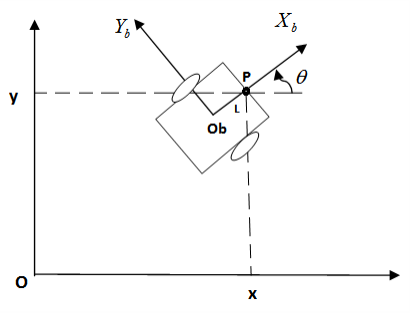

Fig. 2. Schematic of mobile robot. $X_bO_bY_b$ represents the mobile frame.

The UGVs are desired to be placed in a square vertices which is depicted in Fig 3. "a" represents the edge of the square. The center of the formation is determined by the UAV planar position (x,y).

To achieve the desired formation, we utilize feedback linearisation technique. By defining the error for each robot as $e_{xi} = x_i - x_{id}, e_{yi} = y_i - y_{id}$, x_{id} and y_{id} are function of planar position of the UAV (x,y) see Fig2. The control input for mobile robot can be written as:

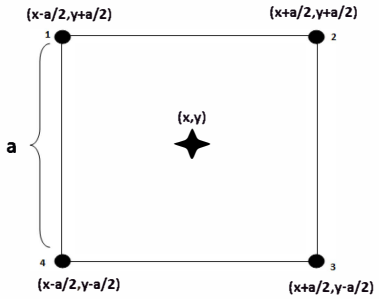

Fig. 3. Desired formation of mobile robots, "a" represents the length of square, (x,y) represents UAV position.

$$\begin{bmatrix} V_{it} \\ \omega_{it} \end{bmatrix} = \begin{bmatrix} cos\theta_i & sin\theta_i \\ \frac{-1}{L} sin\theta_i & \frac{1}{L} cos\theta \end{bmatrix} (-\beta \begin{bmatrix} e_{xi} \\ e_{yi} \end{bmatrix} + \begin{bmatrix} \dot{x_{id}} \\ \dot{y_{id}} \end{bmatrix}) \tag{5}$$

Where β is a gain which determines the rate of convergence. In (5), the subscript "t" is the abbreviation of "tracking".

III. OBSTACLE AVOIDANCE

A. UGV and Obstacle Avoidance

Up to this Section, we could make the mobile robots track the quadrotor in a square shape formation. But, due to UAV field of sight limitation, it is not able to detect small obstacles and the generated path is not free of obstacle. As a result, it is essential to devise an obstacle avoidance algorithm for the UGVs formation.

An important problem in navigation of mobile robots is obstacle avoidance. Several techniques such as neural network, potential field, fuzzy control and so on were introduced in the literature [9]. Among the mentioned approaches, potential field generated by obstacles is so popular. In this techniques when a robot is approaching an obstacle, the repulsive potential field increases and make the robot far from the obstacle ,but if a mobile robot moves in the opposite direction of the potential field, it may stick in a local minima position. Recently a new approach based on limit cycle features is introduced which unlike the conventional potential field does not stick in local minima [9], [10]. This algorithm is employed in this paper. In this algorithm, each obstacle is modeled by its surrounding circle with radius A_c and its position w. r. t global reference frame(x_{ob}, y_{ob}). In order to perform the obstacle avoidance, when an obstacle is sensed, robot should follow the limit cycle trajectory around the obstacle, whose direction is determined based on motion direction of the robot and its relative position to the obstacle. The differential equation describing a limit cycle like movement for UGV, can be written as:

$$\begin{aligned} \dot{x}_{io} &= (-1)^j y_s + \zeta x_s (1 - \frac{{x_s}^2}{{A_c}^2} - \frac{{y_s}^2}{{A_c}^2}) \\ \dot{y}_{io} &= (-1)^{j+1} x_s + \zeta y_s (1 - \frac{{x_s}^2}{{A_c}^2} - \frac{{y_s}^2}{{A_c}^2}) \end{aligned} \tag{6}$$

Where $(x_s = x_i - x_{ob}, y_s = y_i - y_{ob})$, j can be 0,1 that 0 implies a clockwise rotation while 1 stands for a counterclockwise rotation. ζ is a positive constant value. Robot movement is affected by the limit cycle equation until either obstacle will not disrupt the UGV path, or the UGV and obstacle distance is large enough. For more details, refer to [9], [10].

The obtained $\dot{x}_{io}$ and $\dot{y}_{io}$ are employed to find the output of the obstacle avoidance part of the UGVs:

$$\begin{aligned} \omega_{io} &= \frac{-\dot{x}_{io} sin\theta + \dot{y}_{io} cos\theta}{L} \\ V_{io} &= \dot{x}_{io} cos\theta + \dot{y}_{io} sin\theta \end{aligned} \tag{7}$$

To smooth the switching between two control strategies, (5), (7) the following modification is proposed:

$$\begin{aligned} V_i &= V_{io}(\exp(-trsh.mm)) + V_{it}(1 - \exp(-trsh.mm)) \\ \omega_i &= \omega_{io}(\exp(-trsh.mm)) + \omega_{it}(1 - \exp(-trsh.mm)) \end{aligned} \tag{8}$$

Where *trsh* stands for the distance between robot and obstacle and *mm* indicates whether the obstacle is any more placed

in the robot path or not. By drawing a line connecting the robot position and its desired position, if the line does not pass through the obstacle, *mm* is set 100, (which means the obstacle does not disrupt the UGV path) otherwise, *mm* will be 1. V_{it} and ω_{it} are the UGV linear and angular velocities in normal condition, which are calculated by (5).

• ***Remark***

By this control algorithm, the mobile robots do not have to communicate with each other. But, when the UGVs are involved in obstacle avoidance, it is likely that they collide with each other; to avoid this situation, when the mobile robots get near each other, they repel each other. This repulsive force can be written as:

$$if(d_{ij} < d_{min}) \begin{bmatrix} \dot{x_{ica}} \\ \dot{y_{ica}} \end{bmatrix} = \gamma \begin{bmatrix} x_i - x_j \\ y_i - y_j \end{bmatrix} \begin{bmatrix} e_{xi} \\ e_{yi} \end{bmatrix} + \begin{bmatrix} \dot{x_j} \\ \dot{y_j} \end{bmatrix}$$

Where d_{min} stands for the radius of the mobile robot sensing circle. By using formula (17),(18) corresponding robot velocities (V_{ica}, ω_{ica}) obtain.

In conclusion, the mobile robot linear and angular velocity can generally be written as:

$$V_i = V_{io}(\exp(-trsh.mm)) + V_{it}(1 - \exp(trsh.mm)) + \eta V_{ica} \tag{9}$$

$$\omega_i = \omega_{io}(\exp(-trsh.mm)) + \omega_{it}(1 - \exp(trsh.mm)) + \eta \omega_{ica} \tag{10}$$

In eqn (10), η is a function of $\frac{1}{d_{ij}}$ to smooth the agents inputs, for example it can be chosen as $\eta = \frac{1}{d_{ij}} - \frac{1}{d_{min}}$.

B. UGV and UAV distance

When the UGVs are involved in obstacle avoidance, since the aerial vehicle does not detect small obstacles it just tracks the reference trajectory. By increasing the distance between UAV and UGVs their connection quality may deteriorates, to cope this problem, UAV should be aware of its distance with UGVs and keep it in adequate interval. The following assumption is made to facilitate the design of our proposed solution for the mentioned challenge.

• *Assumption.*

The UAV path planner unit commands a path in the following shape:

$$\begin{cases} y_d = f(x_d) \\ if: |\frac{df}{dx_d}| \leqslant U_f \wedge |\frac{dx_d}{dt}| \leqslant U_{dx_d} \Rightarrow |\frac{dy_d}{dt}| \leqslant U_f U_{dx_d} \end{cases} \tag{11}$$

Where U_f is the upper bound for f(.) gradient with respect to x_d and U_{dx_d} is the upper bound for the x_d time derivative. By decreasing U_{dx_d} the upper bound of $\dot{y}$ decreases, too. Therefore, if $U_{dx_d} \propto \frac{1}{d_{ua}}$, (d_{ua} represents the distance between UAV and center of mobile robots formation), as the d_{ua} increases, the UAV velocity decreases. As a result, the d_{ua} remains bounded. This idea can be formulated as:

$$if(d_{ua} \geq d_n) \qquad U_{dx_d} = (\frac{d_n}{d_{ua}})^k . U_{dx_{d0}} \tag{12}$$

where d_n represents the acceptable distance between UAV and the UGVs. $U_{dx_{d0}}$ shows the ordinary upper bound for x_d time derivative. k is a non-negative constant which affects the reduction rate of UAV velocity, In Fig 4 the effect of "k" on UAV-UGVs distance is depicted.

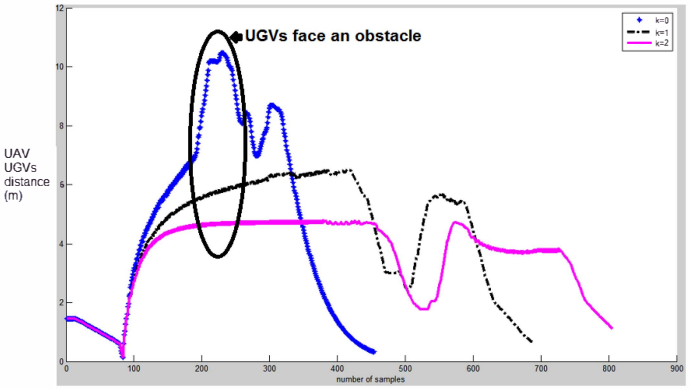

Fig. 4. The effect of k on distance between UAV and Center of UGVs. The circle shows the time when UGVs face an obstacle and are not able to follow UAV. $k = 0$, represents no modification.

C. UAV and Obstacle Avoidance

In this section it is assumed that UAV may encounter pop-up obstacles like birds, micro aerial vehicles and so on. To deal with this problem, we use the limit cycle approach that is already introduced,to the best knowledge of the authors, it is for the first time that limit cycle approach is used for quadrotors to avoid obstacles. Two types of aerial obstacles are considered, namely static and pop-up obstacles.

• ***Static Obstacle***

Let us assume that the path planner unit for the UAV was not able to detect a building, therefore when the UAV is approaching it, UAV sensors recognize it.

For an obstacle in shape of a building or hill, the UAV approximates its dimension. Then by considering a x-y planar limit cycle around the obstacle, the UAV employs the limit cycle based obstacle avoidance algorithm. In this case, the ground robots do not have to care about huge obstacles like building because their leader, UAV, has already considered it.

• ***Pop-up Obstacle***

Imagine a situation in which the quadrotor faces a moving object that is flying at the same height. The UAV can have a vertical movement to avoid the collision. To achieve the desired vertical surface a specific frame with the following features should be defined:

- Consider when the UAV detects the threat at t=t_0, the line which connects the current planar UAV position (x_0,y_0) to the origin of the reference frame, is considered as the "x" axis of new local frame (X_n).
- The X_n connects the origin of the reference frame to the current planar position of the UAV. This axis is oriented toward the current planar position. Actually this frame is achieved by rotation the reference frame around the z axis by θ, see Fig5, where $\theta = atan(\frac{y_0}{x_0})$. The corresponding rotation matrix can be written as

$$R = \begin{bmatrix} cos\theta & -sin\theta & 0 \\ sin\theta & cos\theta & 0 \\ 0 & 0 & 1 \end{bmatrix} \quad (13)$$

$$\begin{bmatrix} x_n \\ y_n \\ z_n \end{bmatrix} = R \begin{bmatrix} x \\ y \\ z \end{bmatrix} \quad (14)$$

Using the equation (6), $\dot{x}_n$, $\dot{z}_n$ are obtained, since the UAV is moving on the zOx surface, we conclude that $\dot{y}_n = 0$. Since the elements of R are constant, corresponding $\dot{x},\dot{y},\dot{z}$ can easily be calculated by inverse kinematic.

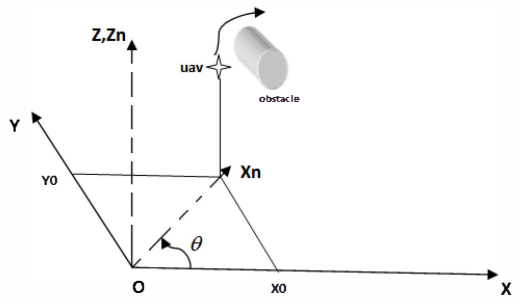

Fig. 5. Illustration of θ in the rotation matrix R, the UAV should move on Z_nOX_n surface to avoid collision,Y0 and X0 represent the UAV position when it detects the pop-up obstacle

• ***Remark***

When UAV faces a pop-up obstacle, it moves on a vertical surface to heighten, as explained. After reaching a safe height, if there is vertical distance constraint between UAV and the UGVs, UAV should return to its previous attitude, otherwise the UAV controller switches to reference path tracking.

IV. SIMULATION RESULTS

The proposed approaches are evaluated by the following scenarios. In all of them the parameters in TableI are used:

•*Case 1*

Consider a multi agent system consisted of 4 mobile robots with dynamics expressed in (4) whose initial positions are (4,0), (0,4), (-2,2),(1,-1) and a quadrotor described in (1) with initial states(x=0, y=0, z=4, $\phi = \pi/4$, $\psi = \pi/4$,$\theta = \pi/4$). The UAV has to track the prescribed path (x_d=y_d, x_d=3t, ψ_d = 0). The ground robots should make a square formation by length of 1 m. There are 2 ground obstacles placed in (15,15), (30,30). Both of them are circles R_{ob}=0.5 m in diameter. The simulation results are depicted in Fig 6, 7, 8. As you can see in the Fig 6, when the distance between UAV and UGVs rises due to ground obstacles, according to (12) the upper bound of $\dot{x}_d$ reduces to prevent from mission failure.

•*Case 2*

In this example, the reference trajectory for UAV is (y_d=3t, x_d=3t+sin(2t), $\psi_d = 0$). Furthermore, we assume in addition to ground obstacle placed in (15,15), there exists an obstacle in shape of tube whose center is placed in (25,25). The obstacle

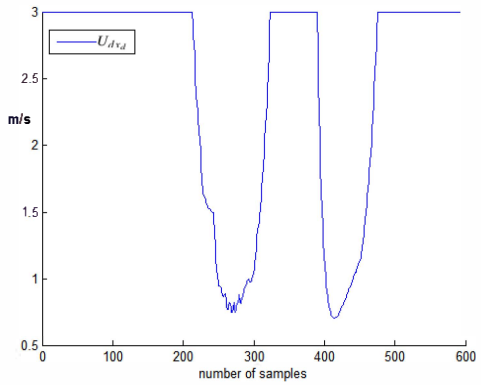

Fig. 6. Reduction in U_{dx_d} by rise in UAV and UGVs distance

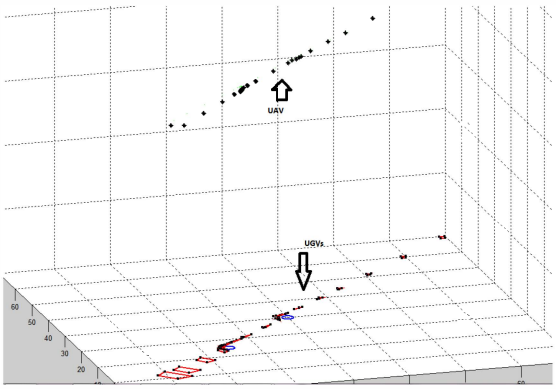

Fig. 7. Case 1, the ⋆ shows the UAV position following the specified trajectory, UGVs track the UAV. In addition, UGVs have to pass the obstacles.

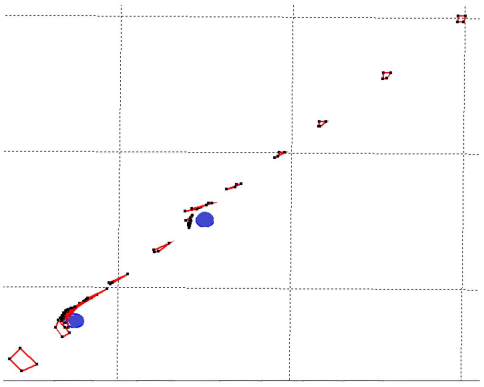

Fig. 8. Case 1, when UGVs are tackling the obstacle the formation is destroyed and by passing the obstacle, the formation revives again. UGVs are depicted as black dots and lines connect the UGVs to show the formation status.

is modeled by a cylinder that is 5 m tall and its base is a circle with 4 m in diameter. It was mentioned, the UAV should move on a planar (XOY) surface because in this example, the UGVs are in danger of collision as well as UAV, see Fig 9.

•*Case 3*

In the last case, the desired trajectory for UAV is (x_d=y_d, x_d=3t, $\psi_d = 0$). In addition to ground obstacles, there exists a

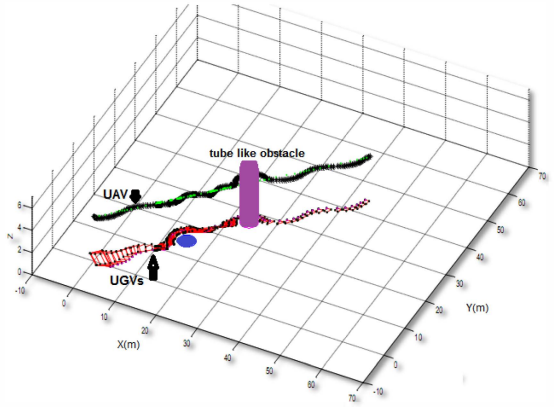

Fig. 9. Case 2, the multi agent system and a tube shape obstacle, the UAV moves on a horizontal surface to avoid the obstacle.

pop-up aerial threat in shape of sphere whose radius is about 2 m. it is moving by on the line $y(t) = -x(t) + 50, x(t) = 3t - 3.2$ The quadrotor moves on the vertical surface as described in previous section. It can be seen in the Fig 10 that when UAV gets to a safe height, the obstacle avoidance algorithm stops. Fig 11 depicts distance between UAV and pop up threat in two cases: with and without obstacle avoidance algorithm.

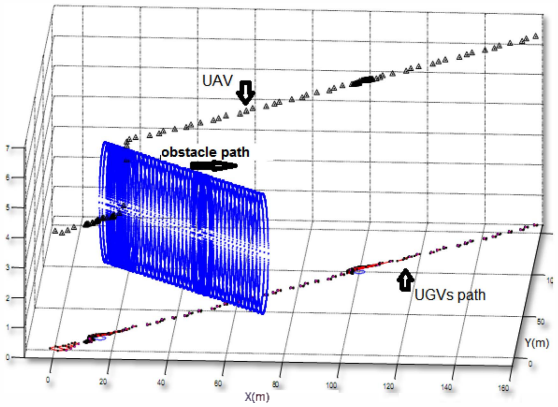

Fig. 10. Case 3, the UAV faces a moving object.The arrow shows the obstacle path. UAV moves on a vertical surface to pass the pop-up threat.

TABLE I
PARAMETER

Parameter	Value(SI)	Parameter	Value(SI)
J_r	3.36e-5	l	0.2
b	2.92e-6	d	1.12e-7
I_z	8.81e-3	g	9.81
I_x	4.85e-3	I_y	4.85e-3
β	0.3	R_{ob}	2
d_{normal}	2	d_{min}	0.2
a(length of desired square)	1	length of mobile robot	0.2

V. CONCLUSION

This paper addresses the cooperation between two types of heterogeneous robots: UAV and UGV. The robots should catch a target which is known for UAV due to its ability

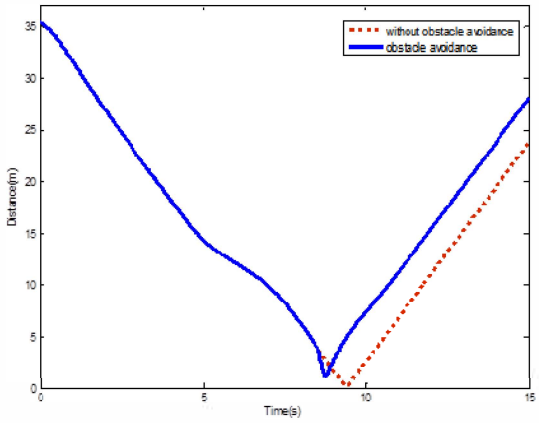

Fig. 11. Case 3, distance between UAV and obstacle. solid line represents the distance when using obstacle avoidance algorithm and dashed one shows the distance with out any obstacle avoidance method.

to observe far distances. As a result, the UAV is considered as leader. On the other hand, the UGVs should keep the desired formation while avoiding possible obstacles. Limit cycle potential field strategy is employed for obstacle avoidance. During obstacle avoidance, UAV improves its motion to keep connection among vehicles. Finally obstacle avoidance algorithm is proposed for large obstacles which both UAV and UGVs should avoid.

REFERENCES

[1] L. Consolini, F. Morbidi, D. Prattichizzo, and M. Tosques, "Stabilization of a hierarchical formation of unicycle robots with velocity and curvature constraints," *IEEE Transactions On Robotics*, vol. 25, no. 5, pp. 1176-1184, 2009.

[2] L. Consolini, F. Morbidi, D. Prattichizzo, and M. Tosques, "Leader-follower formation control of nonholonomic mobile robots with input constraints," *Automatica*, vol. 44, no. 5, pp. 13431349, 2008.

[3] B. Grocholsky, J. Keller, V. Kumar, and G. Pappas, "Cooperative air and ground surveillance,"*IEEE Robotics and Automation magazine*, pp. 16-26, 2006.

[4] N. Ayanian, and V. Kumar, Decentralized feedback controllers for multiagent teams in environments with obstacles, *IEEE Transactions on Robotics*, vol. 26, no. 5 ,pp. 878-887, 2010.

[5] H. G. Tanner, and D. K. Christodoulakis, "Decentralized cooperative control of heterogeneous vehicle groups,"*Robotics and Autonomous systems*, vol. 55, pp. 811-823, 2007.

[6] N. Michael, J. Fink, and V. Kuamr, Controlling a team of ground robots via an aerial robot," *in Proceedings of the IEEE/RSJ International Conference on Intelligent Robots and Systems*, (USA), October ,2007, pp. 965-970,.

[7] A. Das, K. Subbarao, and F. Lewis, "Dynamic inversion with zero-dynamics stabilisation for quadrotor control," *IET control theory and application*, vol. 3, pp. 303-314, 2009.

[8] S.Bouabdallah, and R. Siegwart, "Backstepping and sliding mode techniques applied to an indoor micro quadrotor", in Proceedings of the *International Conference on Robotics and Automation*, (Spain), 2005, pp. 2247-2252.

[9] H. Rezaee, and F. Abdollahi, "Mobile robots cooperative control and obstacle avoidance using potential field," in Proceedings of the *International Conference on Advanced Intelligent Mechatronics*, (Hungry), July 2011, pp. 61-66.

[10] L. Adouane, A. Benzerrouk, and P. Martinet, "Mobile robot navigation in cluttered environment using reactive elliptic trajectories", in Proceedings of the 18^{th} *IFAC World Congress*, (Italy), August 2011, pp. 13801-13806.